

## Asymptotic dynamics of breathers in Fermi-Pasta-Ulam chains

R. Reigada,\* A. Sarmiento,† and Katja Lindenberg

*Department of Chemistry and Biochemistry and Institute for Nonlinear Science, University of California San Diego, 9500 Gilman Drive, La Jolla, California 92093-0340*

(Received 14 May 2002; revised manuscript received 23 July 2002; published 10 October 2002)

We carry out a numerical study of the asymptotic dynamics of breathers in finite Fermi-Pasta-Ulam chains at zero and nonzero temperatures. While at zero temperature such breathers remain essentially stationary and decay extremely slowly over wide parameter ranges, thermal fluctuations tend to lead to breather motion and more rapid decay. In both cases the decay is essentially exponential over long time intervals.

DOI: 10.1103/PhysRevE.66.046607

PACS number(s): 05.40.-a, 05.45.-a, 63.20.Pw

### I. INTRODUCTION

Energy localization in the form of breathers has been intensely investigated over the past several years [1]. These highly localized long-lived excitations in translationally invariant nonlinear arrays are of great interest because they provide a mechanism for energy storage that does not rely on defects. The fact that these excitations are often mobile makes them particularly interesting in the context of efficient transport of vibrational energy [2].

Breather excitations that persist forever can be confirmed analytically and constructed numerically for certain nonlinear arrays, among them infinite arrays of masses with interactions between neighboring sites that vary as  $(x_i - x_j)^n$  with  $n \rightarrow \infty$  [3]. The  $x$ 's denote displacements of the masses at sites  $i$  and  $j$ . When the interactions are not precisely of this form, or when the array is finite, or when other excitations (for example, phonons or other localized excitations) are present, it is no longer possible to prove exact breather solutions. Nevertheless, it is possible to explore the problem numerically. In this report we study the asymptotic dynamics of breathers in the one-dimensional Fermi-Pasta-Ulam (FPU)  $\beta$  model at zero temperature and during thermal relaxation.

We corroborate that long-wavelength thermal excitations have a profound effect on breather stability. In particular, our work supports three main conclusions concerning the dynamics of breathers whose frequencies are initially much higher than phonon frequencies in FPU  $\beta$ -chains: (1) At zero temperature in finite chains, breather excitations remain localized, and their energy (and that of the entire chain) decays essentially *exponentially* until their frequency approaches that of the phonon band, whereupon the final decay is very rapid. (2) The exponential decay time  $\tau$  at zero temperature is extremely long compared to phonon decay times. (3) Thermal background, especially long wavelength background, keeps the breather in motion, which in turn leads to its more rapid decay. These results extend our earlier work to much

longer time regimes [4], and agree with and complement those of Piazza *et al.* [5].

The paper is organized as follows. In Sec. II we present numerical results for chains initially at zero temperature, and explore the dependence of the dynamics on various system parameters. In Sec. III we discuss breather decay in chains initially at a finite temperature. We end with a summation in Sec. IV.

### II. BREATHERS AT ZERO TEMPERATURE

The Hamiltonian for the FPU  $\beta$  model is

$$H = \sum_{i=1}^N \frac{\dot{x}_i^2}{2} + \frac{k}{2} \sum_{i=1}^N (x_i - x_{i-1})^2 + \frac{k'}{4} \sum_{i=1}^N (x_i - x_{i-1})^4, \quad (1)$$

where  $N$  is the number of sites, and  $k$  and  $k'$  are the harmonic and anharmonic force constants, respectively. We set  $k = k' = 0.5$  throughout. The relative values of the two constants can be shifted by rescaling space and time. In particular, by introducing new variables  $y_i = \alpha x_i$  and  $\tau = t/\alpha$ , where  $\alpha$  is a scaling constant, one finds that the scaled Hamiltonian  $\alpha^4 H$  in the new variables is again of the form (1) but with coupling constants  $\alpha k$  and  $k'$ . The results are therefore related through appropriate scaling for any choice of coupling constants *provided neither is zero* [4]. The equations of motion with free-end boundary conditions are integrated using a fourth order Runge-Kutta method with time interval  $\Delta t = 5 \times 10^{-4}$  (further reduction leads to no significant improvement) [6]. The total energy  $\varepsilon(t)$  of the array is the sum over individual symmetrized site energies  $E_i(t)$  [4]. A zero temperature environment with the least disturbance to the dynamics in the chain is achieved by connecting the chain ends to such an environment via a dissipation term, that is, by adding  $-\gamma \dot{x}_i$  to the equations of motion for sites  $i = 1$  and  $i = N$  [4,5].

In order to observe breather decay, we begin by creating an “odd parity” excitation with amplitudes  $-A/2$ ,  $A$ , and  $A/2$  on three successive sites, zero amplitude on the other sites, and zero velocity at each site. We identify this excitation as *the breather* and thereby distinguish it from other excitations that emerge during the relaxation process. The predominant frequency of the breather is higher for higher  $A$ , which must be chosen so that this frequency is well above

\*Permanent address: Departament de Química Física, Universitat de Barcelona, Avda. Diagonal 647, 08028 Barcelona, Spain.

†Permanent address: Instituto de Matemáticas, Universidad Nacional Autónoma de México, Ave. Universidad s/n, 62200 Chamilpa, Morelos, Mexico.

the phonon band edge at  $\omega = \sqrt{4k} = \sqrt{2}$  in order to avoid rapid decay by phonon radiation. This excitation is not an exact stationary solution of the equations of motion, so it typically sheds some energy (thereby “warming” the chain) while reaccommodating amplitudes and lowering its frequency [4], and settles into a very long-lived excited configuration which continues to discard energy until it eventually disintegrates. A measure of the magnitude of the chain relaxation times reported below is obtained by recalling that phonons of a given wave vector  $q$  decay exponentially with a decay time that depends on  $q$ , and that the shortest-wavelength phonons have the longest decay times,  $\tau_{ph} \sim N^2/\gamma$  [5].

The discarded energy appears in the form of lower-energy localized excitations and/or phonons. The precise subsequent evolution depends on a number of parameters: the initial amplitude  $A$ , the chain length  $N$ , the damping parameter  $\gamma$ , and the location of the center of the initial excitation. Before pursuing some specific parameter dependence trends in more detail, we note the following. As mentioned above, we establish numerically that the decay of the breather is essentially exponential over long time intervals. However, the actual decay time depends (among other factors) on the breather amplitude, being larger for larger amplitudes (see below). Therefore, even as the breather slowly loses energy, its amplitude decreases and consequently its decay rate slowly increases, that is, the “decay time”  $\tau$  is itself mildly time dependent, until the breather frequency approaches the phonon band edge and the breather disintegrates rapidly into phonons. Thus the time dependence of  $\tau$  is slower for more energetic excitations. The total lifetime of the breather is bounded above by the very slow decay time at its highest amplitude and the phonon lifetimes into which it eventually disintegrates.

Consider the following specific scenario, which serves to establish the way in which we extract relevant relaxation times from our numerical results. We create an odd-parity excitation of amplitude  $A$  exactly in the middle of the chain of  $N=31$  sites, and set the end-site dissipation parameter  $\gamma = 1$ . The breather discards some energy that travels toward the chain ends and dissipates quickly, in a time  $\tau_m$ , across the ends of the chain. The remaining energy stays localized in the middle of the chain, most of it (98% for  $A=0.5$ ) on the three initially excited sites, and decays exponentially with an extremely long characteristic time  $\tau$  (for a discussion of the relative stability of breathers of different configurations see [7]).

To extract exponents and characteristic times, it is important to gather data that covers both time scales, and to normalize the data in such a way that one behavior does not mask or distort the other [8]. We introduce the *normalized energy*  $E(t)$  and the *modified normalized energy*  $E_m(t)$  as follows:

$$E(t) = \frac{\varepsilon(t)}{\varepsilon(0)}, \quad E_m(t) = \frac{\varepsilon(t)}{\varepsilon(\tau_m)}. \quad (2)$$

The denominator in the first contains the initial energies, and in the second the energies after the discarded low energy

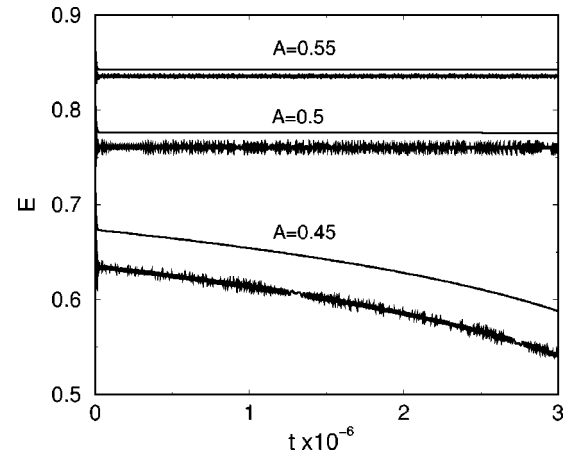


FIG. 1. Decay of the normalized energy  $E(t)$  for three different values of the initial amplitude  $A$  for chains of  $N=31$  sites connected at the ends to a zero-temperature bath. The breather is located at the center of the chain. The dissipation parameter  $\gamma=1$ . The thin lines represent the total energy remaining in the chain, and the bold lines the portion of the remaining energy that is localized on the three initially excited sites.

excitations have dissipated (but before the remaining breather has decayed appreciably). In this illustration we take  $\tau_m = 40,000 \geq \tau_{ph}$ .

In Fig. 1 we show typical results for  $E(t)$  for three excitation amplitudes over more than six decades of time. The modified normalized energy follows essentially the same behavior. If the decay of the long-lived excitation is exponential, we expect  $[-\ln E(t)]$  and  $[-\ln E_m(t)]$  vs  $t$  to be straight lines over appropriately long time intervals. In Fig. 2 we clearly see this behavior, which extends over the entire time interval for the higher amplitude excitation. The slope for the  $A=0.5$  curve leads to a decay time of  $\tau = 2.80 \times 10^9$ , a specific number reported here principally to stress its enormous magnitude compared to  $\tau_{ph}$ . The change in slope of the curve associated with the lower amplitude breather captures the slow change in the decay rate as the breather frequency edges toward the phonon band. Here we also see clearly that the more energetic breather relaxes more slowly.

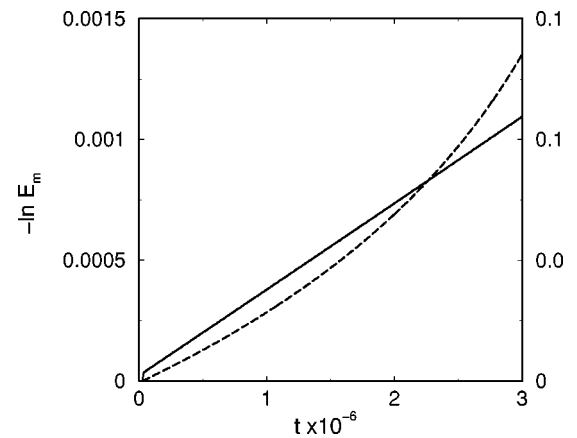


FIG. 2.  $[-\ln E_m(t)]$  vs  $t$  for two initial amplitudes,  $A=0.5$  (solid curve, left scale) and  $A=0.45$  (dashed curve, right scale), for a chain of 31 sites with a breather at the center and  $\gamma=1$ .

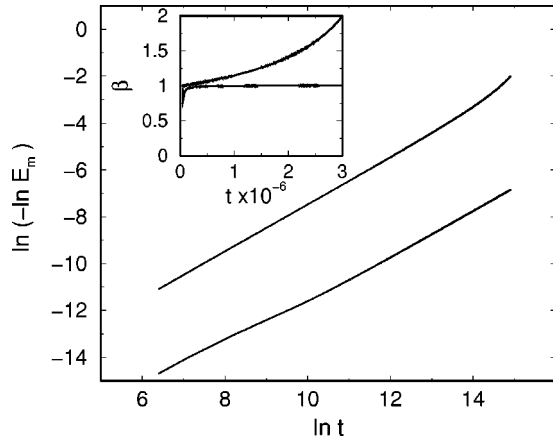


FIG. 3.  $[\ln(-\ln E_m(t))]$  vs  $\ln t$  for two initial amplitudes,  $A = 0.5$  (lower curve) and  $A = 0.45$  (upper curve), for a chain of 31 sites. The inset shows the associated slopes in the same order.

Figure 3 confirms the exponential decay [5,8]. For two initial amplitudes, the figure shows  $[\ln(-\ln E_m(t))]$  vs  $\ln t$ , which yields a straight line of slope  $\beta$  if  $E_m(t) \propto e^{-(t/\tau)^\beta}$ . The inset shows the values of the slopes  $\beta$  as a function of time. For  $A = 0.5$ , pure exponential behavior  $\beta = 1$  is confirmed throughout the time range presented. Approach of the breather frequency to the phonon band edge increases the decay rate, an effect clearly seen for the lower amplitude.

A breather of a given amplitude has a characteristic predominant frequency. In Fig. 4 we show this frequency in relation to the phonon band edge as a function of time for the cases discussed above. For 31-site chains, the frequency of the breather of initial amplitude  $A = 0.5$  decreases very little over the entire simulation, while that of initial amplitude  $A = 0.45$  decreases more markedly. Consistent with the fact that the breather does not disappear entirely in the time range shown, its frequency never reaches the phonon band edge. If the initial amplitude of the excitation were even smaller, or

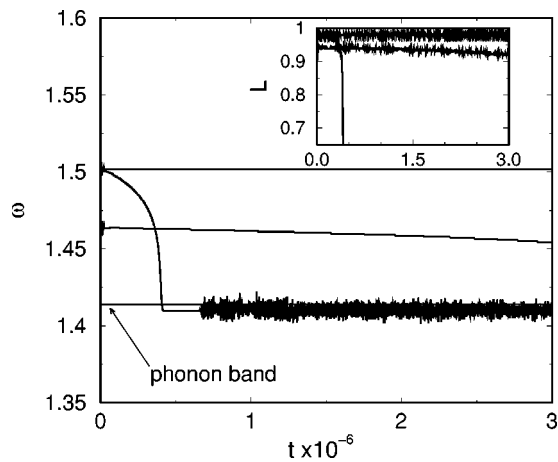


FIG. 4. Breather frequency as a function of time. Curve that persists at the highest frequency ( $\omega \sim 1.5$ ):  $A = 0.5$ ,  $N = 31$ . Curve that begins at  $\omega \sim 1.465$  and decreases gently:  $A = 0.45$ ,  $N = 31$ . Curve that turns sharply downward:  $A = 0.5$ ,  $N = 21$ . Inset: associated localization parameters in the same order.

TABLE I. Relaxation times calculated as described in the text for breathers of increasing initial amplitude for a chain of 31 sites and  $\gamma = 1$ . The breather is located exactly at the center of the chain.

$A$	$\tau_1$	$\tau_2$
0.45	$2.96 \times 10^7$	$1.53 \times 10^7$
0.46	$8.32 \times 10^7$	$6.81 \times 10^7$
0.47	$3.12 \times 10^8$	$2.53 \times 10^8$
0.48	$4.83 \times 10^8$	$4.61 \times 10^8$
0.49	$1.19 \times 10^9$	$1.18 \times 10^9$
0.50	$2.79 \times 10^9$	$2.78 \times 10^9$
0.51	$7.04 \times 10^9$	$7.04 \times 10^9$
0.53	$3.12 \times 10^{10}$	$3.12 \times 10^{10}$
0.55	$1.43 \times 10^{11}$	$1.43 \times 10^{11}$
0.60	$2.81 \times 10^{14}$	$2.81 \times 10^{14}$

the simulation time much longer, or the chain shorter, the breather would be seen to disappear. This last case is illustrated in Fig. 4. The breather disintegrates entirely when its frequency reaches the band edge. The inset shows  $L$ , the ratio of the energy of the five sites centered on the breather, to the total energy.  $L$  is of order unity when most of the energy is localized on a small number of sites. Note that the lifetime of this breather, which is of  $O(5 \times 10^5)$ , is still much longer than the longest phonon lifetime, which is of  $O(10^4)$ .

The above results are typical of one particular scenario: a breather created exactly in the middle of a chain of  $N$  sites whose ends are connected to the zero-temperature bath with dissipation parameter  $\gamma = 1$ . It is interesting to explore qualitative and even quantitative dependences as one changes these conditions. The dependence of the chain energy relaxation times on the initial amplitude of the breather is monotonic. In Table I we exhibit illustrative results for the decay times for breathers of different initial amplitudes in 31-site chains, including those associated with the decay curves shown in Figs. 1–4. The first column gives the initial amplitude of the breather constructed in the middle of the chain with end-site dissipation parameter  $\gamma = 1$ , as before. We stress that the lifetimes of all these breathers are much longer than our total simulation times  $t = 3 \times 10^6$ . The second column shows the decay time, denoted by  $\tau_1$ , obtained from a fit of the slopes such as shown in Fig. 2 over the time span from  $t = 10^6$  to  $t = 2 \times 10^6$ . The third column shows the decay time, denoted by  $\tau_2$ , obtained from the slope over the range  $(2 \times 10^6) - (3 \times 10^6)$ . For the lower amplitude breathers  $\tau_1$  is slightly longer than  $\tau_2$ , indicative of the increase of the breather decay rate as its frequency edges toward the phonon band. For the higher amplitude breathers the decrease is not discernible over our simulation times and the decay is essentially strictly exponential. Eventually their decay will also speed up, but it will occur well beyond the times included in our studies. Clearly, the decay rate decreases sharply with increasing breather amplitude.

The evolution of the breather depends in an interesting way on its initial location and on the damping parameter  $\gamma$  when the latter is either very small or very large. Figure 5 shows the very early evolution (up to  $t = 2000$ ) of a breather initially centered on site 15 of a 31-site chain, that is, slightly

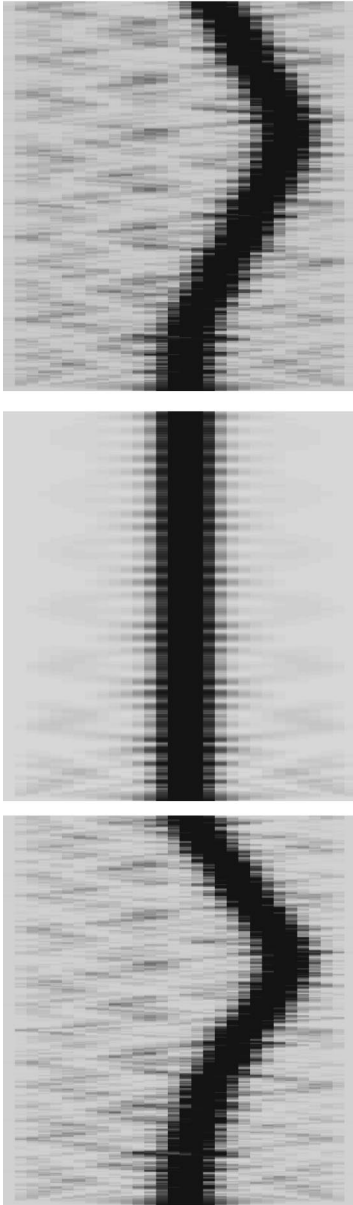


FIG. 5. Energy landscapes of 31-site arrays. The breather of amplitude  $A=0.5$  is initially centered at site 15. Time advances along the  $y$  axis until  $t=2000$ . A gray scale is used to represent the local energy, with darker shading corresponding to more energetic regions. First panel:  $\gamma=0.01$ . Second panel:  $\gamma=1$ . Third panel:  $\gamma=100$ .

off-center, for three values of the damping parameter. The middle panel is for  $\gamma=1$ , the damping we have considered so far. The behavior of the excitation in this panel starts out as we have described it, that is, it sheds some energy (medium-gray scale) that dissipates quickly. Although a small fraction of the energy that has been shed oscillates back toward the breather, it is not sufficient to set it in motion; most of the energy simply moves towards the chain ends and dissipates into the zero-temperature bath. The evolution of the breather proceeds as described earlier for a breather initially centered in the middle of the chain (site 16) with only a small modification of its decay time (see below).

This behavior is fairly robust for values of  $\gamma$  within an order of magnitude on either side of  $\gamma=1$  and for breathers that are excited not too near the chain ends.

The situation is rather different if  $\gamma$  is either very small (first panel) or very large (third panel). The qualitative similarity between these two extreme cases is apparent: the chain ends no longer dissipate the energy that has been shed by the breather as effectively, and so it returns to perturb the breather and set it in motion. In turn, this causes the breather to decay more rapidly into more rapidly dissipated lower-energy excitations [4]. In the very low damping case energy that arrives at the chain ends cannot go anywhere except back, much like a whip. In the very high  $\gamma$  case the end sites are so damped that they can absorb very little energy from the rest of the chain, much like a wall. We have followed these particular histories over our usual time span of 3 million time units and find the decay times  $\tau_1 \approx \tau_2 = 1.56 \times 10^9$  for  $\gamma=1$ ,  $\tau_1 = 1.90 \times 10^6$  and  $\tau_2 = 1.22 \times 10^6$  for  $\gamma=0.01$ , and  $\tau_1 = 3.45 \times 10^7$  and  $\tau_2 = 3.12 \times 10^7$  for  $\gamma=100$ . The trend is thus as described; the particular values are susceptible to change depending on the initial location of the breather and the values of the other parameters of the system.

It should be pointed out that an odd parity breather initially centered *exactly* in the middle of the chain constitutes a rather singular case when damping is very low or very high, with relative decay rates *opposite* to those reported above. While the  $\gamma \sim 1$  results are not much affected by the initial location of the excitation (provided it is far from the chain ends), in this peculiar case the extreme- $\gamma$  cases lead to *slower* decay than for  $\gamma \sim 1$ . In this unique case, the symmetry of the problem leads to the breather being buffeted from both sides by *identical* energy pulses that return from the ends of the chain. In the absence of symmetry breaking, the breather is therefore not set in motion, and instead simply re-absorbs this energy (and reemits and reabsorbs energy in increasingly smaller amounts). Since the energy that returns from the chain ends is greater in the extreme  $\gamma$  cases than it is for intermediate  $\gamma$ , the chain energy remains higher, and the decay is thus slower.

Breather decay times are strongly dependent on the chain length: the decay times increase markedly, as does the total lifetime of the breather, with increasing  $N$ . This is already apparent when one compares the  $N=31$  and  $N=21$  results in Fig. 4. Whereas a breather of initial amplitude  $A=0.5$  created at the center of a 31-site chain has barely decayed over 3 million time units, a breather of the same initial amplitude in a 21-site chain has disintegrated completely well before that. With  $A=0.5$  and  $\gamma=1$  for the centered breather we find, with  $\tau = \tau_1 = \tau_2$  the values  $\tau = 2.80 \times 10^9$  for  $N=31$  (as reported above),  $\tau = 3.21 \times 10^{12}$  for  $N=41$ , and  $\tau = 3.60 \times 10^{15}$  for  $N=51$ . This behavior is entirely reasonable since the decay of the breather is intimately connected with the presence of a background of other excitations disturbing the breather and the effects of the damped chain boundary sites. All else being the same, both of these are reduced in longer chains. Extremely long simulations runs are necessary to quantify the  $N$  dependence for even longer chains; such a

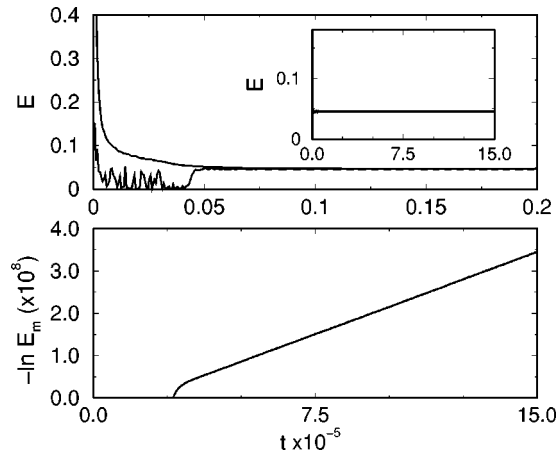


FIG. 6. Upper panel: the smooth curve is the normalized energy as a function of time for a chain of 30 sites initially thermalized at  $T=0.5$  and connected through its ends to a zero-temperature heat bath ( $\gamma=0.1$ ). The initially jagged curve is the normalized energy on sites 13, 14, 15, and 16. The inset shows the temporal evolution of the energy on these four sites over a longer time scale. Lower panel:  $[-\ln E_m(t)]$  vs  $t$  for the same chain.

study, together with an analysis of the effects of different boundary conditions, will be pursued in more detail elsewhere [9].

Pure exponential decay indicates that there is a single rate-limiting decay channel for the energy [4]. This channel is the shedding of energy in the form of phonons and/or lower energy localized excitations by the breather. The degradation of lower-energy localized excitations, and the dissipation of energy into the zero-temperature bath, are much faster processes. The shedding process is slower for longer chains and more energetic breathers of frequencies farther from the phonon band, since the localized excitation is then closer to an exact stationary solution.

### III. BREATHERS AT FINITE TEMPERATURES

When a localized excitation evolves in a thermal environment, other excitations in the medium perturb the breather, and its eventual fate varies from one realization to another. To illustrate the complexity of the situation, we present two scenarios.

We begin with a chain that is initially in thermal equilibrium at a nonzero temperature [4]. At time  $t=0$ , the end sites of the thermalized chain are connected to a zero temperature bath via purely dissipative terms [4,5,10]. We follow the thermal relaxation of the chain and, in particular, the dynamics of breathers that are likely to appear anywhere during relaxation if the initial temperature is sufficiently high. Figure 6 shows the evolution of the normalized energy in a chain of 30 sites initially thermalized at temperature  $T=0.5$ , as well as the energy in only the four sites  $i=13,14,15,16$ . After a relatively short time (5000 time units in this particular realization) almost all of the energy settles in these sites and remains there. The excitation around the four sites turns out to be an “even parity” breather, with maximum displacements  $A$  and  $-A$  alternating on sites 14

and 15, smaller but not negligible amplitudes at sites 13 and 16, and essentially no motion of the other sites. The breather is coincidentally at the center of the chain, but may appear anywhere in different realizations, particularly in longer chains. The frequency of the breather, initially  $\omega=1.633$ , decreases very little for the duration of the simulation. We also present the modified normalized energy, whose decay is clearly exponential, with an enormously long time constant,  $\tau=3.5 \times 10^{13}$ . Thus this breather, even in our relatively short chain, is essentially stationary. This decay time is much longer than that reported in the previous section, consistent with the fact that the amplitude of the breather that has emerged spontaneously is larger. The thermal relaxation process has swept the lattice clean of all other excitations, allowing the breather to survive undisturbed [4]. In our earlier work we reported a stretched exponential rather than a purely exponential decay, a conclusion that relied on the normalized rather than the modified normalized energy [8], on a time history that was not sufficiently long, on a statistical average over a thermal ensemble that included realizations where breathers appeared at different locations (which, as we have seen, might affect decay rates), and also realizations where no breather appeared during the thermal relaxation process (and where the energy dissipation was consequently much more rapid).

In our second scenario, at  $t=0$  a breather of the same amplitude  $A$  as in the first scenario is explicitly injected into a chain that is in thermal equilibrium at a very low temperature (low in the sense that the spontaneous formation of breathers is highly unlikely). The chain is then allowed to relax into a zero temperature heat bath. We find that the thermal background invariably sets the breather in motion, and causes the breather to collide with other excitations and with the chain boundaries. Collision events not only cause the breather to keep moving, but also lead to breather degradation through loss of energy upon collision [4]. The resulting decay of the breather is then in general much faster than in the first scenario. The decay time is also much smaller than that of a breather of the same amplitude injected into a zero temperature chain. We find this behavior even when the temperature is extremely low (all the way down to  $T=10^{-7}$ ). As a quantitative check we have explicitly injected a breather of initial amplitude  $A=0.5$  into a chain thermalized at  $T=10^{-6}$ , that is then allowed to relax into a zero temperature bath. Compared to the zero temperature case, the decay time of the breather is now much reduced,  $\tau=1.32 \times 10^6$ . A similar comparison with  $A=0.55$  again leads to dramatically different decay times,  $\tau=1.43 \times 10^{11}$  ( $T=0$ ) and  $\tau=2.12 \times 10^6$  ( $T=10^{-6}$ ). Note that it does not much matter whether the injected breather is of even or odd parity (here we have injected an odd one).

Why is a breather created spontaneously during thermal relaxation more stable than one explicitly injected into a thermalized chain, even at extremely low temperatures? The answer lies in the effect of different phonons on breather dynamics [4,5]. Whereas short wavelength zone-boundary phonons contribute to spontaneous breather formation (“modulational instability”), breathers are most strongly perturbed and degraded by the longest wavelength phonons.

These are also the phonons that dissipate most rapidly out of a chain with free-end boundaries into a zero-temperature bath [5]. In the higher temperature system, when the breather is created spontaneously the long wavelength phonons have already dissipated and, as dissipation continues up the phonon spectrum, the breather is increasingly less disturbed until it reaches a spatially stationary very long-lived configuration [4]. On the other hand, if the breather is injected into a thermalized system, the breather is subject to strong disturbance by long wavelength phonons even at the very lowest temperatures until these phonons dissipate. In chains undergoing thermal relaxation, an injected breather in the thermalized scenario is therefore a more fragile excitation than a spontaneously created breather of the same amplitude. To confirm this description we have followed the dynamics of a breather injected into a relaxing chain *after* the long wavelength phonons have decayed, and find the breather to be almost as stable as one in a zero-temperature simulation. For example, for a zero-temperature injected breather of initial amplitude  $A=0.6$  in a chain of 31 sites ( $\omega=1.65$ ), we find  $\tau=2.81 \times 10^{14}$ . In a chain initially thermalized at  $T=10^{-5}$  and then allowed to relax, if we wait until  $t=15\,000$  before injecting the same breather we find a somewhat shortened but still very long decay time of  $\tau=5.92 \times 10^{13}$ , in any case much longer than it would be if injected at  $t=0$ . We have also observed a breather in a chain whose temperature is maintained at an extremely low but nonzero value. The breather in this case is always fragile, continuing to move and lose energy until it degrades completely. The zero temperature stability of the breather is therefore a somewhat singular result.

#### IV. SUMMATION

Our work supports the assertions concerning the dynamics of breathers in FPU  $\beta$  chains stated in our Introduction, which indicate that breathers in a zero-temperature environment relax very slowly compared to phonon dissipation

times, that effects of thermal fluctuations must be taken into account even at extremely low temperatures, and that zero-temperature results are in some ways fragile. We have confirmed that breather decay for any particular realization is essentially exponential [5], with a slowly varying decay rate until the breather frequency closely approaches the phonon band edge, whereupon the breather quickly disintegrates. We have uncovered a number of trends and dependences of the breather decay rate. Among them, we have noted the effects on breather decay times of breather amplitude/frequency, damping coefficient at the ends of the chain, initial location of the breather, and chain length. We have confirmed that the drastic increase in the breather decay rate caused by a thermal background is overwhelmingly due to long-wavelength phonons. Absent these phonons, the presence of shorter wavelength excitations leads to only a mild reduction in the breather decay time. We have noted that exponential decay indicates a single rate-limiting decay channel [4], which we have identified as the shedding of energy by the breather in the form of phonons and/or lower energy localized excitations. However, an ensemble averaged decay would reflect the variations of the characteristic exponential decay time of each realization and might in general not even be of purely exponential form. Finally, it would be interesting to extend earlier work on arrays with nonlinear *on-site* potentials [10] to consider some of the detailed issues examined herein.

#### ACKNOWLEDGMENTS

The authors are grateful to F. Piazza for enlightening discussions. This work was supported by the Engineering Research Program of the Office of Basic Energy Sciences at the U. S. Department of Energy under Grant No. DE-FG03-86ER13606. Support was also provided by a grant from the University of California Institute for México and the United States (UC MEXUS) and the Consejo Nacional de Ciencia y Tecnología de México (CONACYT).

- 
- [1] A.J. Sievers and S. Takeno, Phys. Rev. Lett. **61**, 970 (1988); S. Aubry, Physica D **103**, 201 (1997); S. Flach and C.R. Willis, Phys. Rep. **295**, 181 (1998); Physica D **119**, 237 (1999); D. Hennig and G.P. Tsironis, Phys. Rep. **397**, 334 (1999); R.S. MacKay, Physica A **288**, 174 (2000); M. Peyrard and J. Farago, *ibid.* **288**, 199 (2000); P.G. Kevrekidis, K.O. Rasmussen, and A.R. Bishop, Int. J. Mod. Phys. B **15**, 2833 (2001).
- [2] G. Kopidakis, S. Aubry, and G.P. Tsironis, Phys. Rev. Lett. **87**, 165501 (2001).
- [3] S. Flach, Phys. Rev. E **51**, 1503 (1995); J.L. Marin and S. Aubry, Nonlinearity **9**, 1501 (1996).
- [4] R. Reigada, A. Sarmiento, and K. Lindenberg, Phys. Rev. E **64**, 066608 (2001); Physica A **305**, 467 (2002).
- [5] F. Piazza, S. Lepri, and R. Livi, J. Phys. A **34**, 9803 (2001).
- [6] Stability of the integration has been checked in isolated chains. For the breather amplitudes considered here,  $A \leq 0.6$ , the total energy remains constant to 10 or more significant figures over at least  $3 \times 10^6$  time units. Stability problems with the fourth order Runge-Kutta method and the discretization time interval  $\Delta t$  do begin to emerge for larger breather amplitudes.
- [7] J.B. Page, Phys. Rev. B **41**, 7835 (1990); K.W. Sandusky, J.B. Page, and K.E. Schmidt, *ibid.* **46**, 6161 (1992); Y.S. Kivshar *et al.*, *ibid.* **58**, 5423 (1998).
- [8] F. Piazza (private communication).
- [9] R. Reigada *et al.* (in preparation).
- [10] G.P. Tsironis and S. Aubry, Phys. Rev. Lett. **77**, 5225 (1996); A. Bikaki, N.K. Voulgarakis, S. Aubry, and G.P. Tsironis, Phys. Rev. E **59**, 1234 (1999).